Application of the GIS based multi-criteria decision analysis and analytical hierarchy process (AHP) in the flood susceptibility mapping (Tunisia)

Salma Hammami[1] · Lahcen Zouhri[2] · Dhekra Souissi[1] · Ali Souei[3] · Adel Zghibi[1] · Amira Marzougui[4] ·
Mahmoud Dlala[1]

Abstract

Flooding is considered as the most dangerous natural catastrophe in the world. This paper develops a spatial multi-criteria decision production prototype for the evaluation of flooding susceptibility for the city of Tunis. Eight criterions were considered in order to identify and assess the spatial distribution of hazardous zones and were integrated in the Geographical Information System (ArcGIS). The analytical hierarchy process (AHP) is a mathematical technique for flood hazard modeling and decision support based on the weight and rank of each flood factor in order to calculate Flood Hazard Index (FHI) to generate a flood susceptibility map. This was classified from very low to very high classes flood potential. Five classes are observed: 2.85% (very low), 7.5% (low), 17.95% (moderate), 20.63% (high), and 51.06% (very high). FHI was coupled with a sensitivity analysis to derive the Flood Hazard Index with sensitivity (FHIS). This index evaluates the effect of each criteria which allows for better assessment of the role of each parameter in flood susceptibility. The results of this study provide a basis to limit the impacts of flood and protect urban zone against inundation.

Keywords Flood susceptibility · Multi-criteria decision · Arc-GIS · AHP · Sensitivity analysis · Tunisia

Introduction

A flood or inundation can be generally defined as an overflow of water that submerges land that is usually dry. It occurs rapidly, generally within 1 h of rainfall, and sometimes accompanied by landslides, mudflows, bridge collapse, damage to buildings, and fatalities (Hapuarachchi et al. 2011).

✉ Salma Hammami
salmahammami11@hotmail.com

1. UR13ES26, Paléoenvironnement, Géomatériaux et Risques Géologiques, Faculté des sciences de Tunis, Université de Tunis El Manar, 2092 Tunis, Tunisia

2. AGYLE, SFR Condorcet FR CNRS 3417, UniLaSalle, 19 Rue Pierre Waguet, 60026 Beauvais, France

3. Georesources Laboratory, Water Reseaches and Technology Center (CERTE), Tunis El Manar University, 2092 Tunis, Tunisia

4. Institut National Agronomique de Tunisie, Université de Carthage, 1082 Tunis, Tunisia

Flooding is considered as the most frequent natural disasters during the last decades (Rahmati et al. 2016a, b). The frequency of such natural catastrophe is growing each year (Ushiyama et al. 2017), and results from several factors including climate change, urbanization, population growth, the partial or total cover of watercourse by construction of roads or other structures, and unsuitably dimensioned rainwater drainage channel (Green et al. 2000). Floods impact both socioeconomic and environmental attributes of the affected area (Meyer et al. 2013). Tunis has suffered floods regulary since 1969, caused by land use changes and climate variability. The most violent one was in 2003 and in 2017 whose immediate impacts included loss of human life, the destruction of infrastructures, and damage to property. The areas of Ettadhamen, Ettahrir, Ariana, and Ksar Saïd regions which are located in the Tunis were the worst hint. To date, the infrastructure damage due to flooding causes the intermittent supply of water and poor service delivery of wastewater treatment, transport, electricity, education system, communication network, and health care. Reduction in purchasing power in the floodplains can leave communities economically vulnerable.

Studies to improve stormwater sanitation and flood protection have already been carried out since 1966, including the DHU's Flood Protection Study launched by DHU and the Japan Cooperation Agency on 1994. Unfortunately, many developments proposed in these studies have not been fully implemented and some projects have negative impacts related to undersizing rainwater channels, or underestimation of hydraulic parameters (DHU 2015).

The 2003 floods showed the limits of the infrastructure and its inability to protect the population against the socioeconomic damage and against the environmental impact. Therefore, it is necessary to assess the flood risk by adopting the appropriate tools in the study area.

Flood risk assessment has been studied by several authors such as Arrighi et al. 2018, Benson et al. 2016, Ortiz et al. 2016, and Shankman and Keim 2016. In the past decades, numerous techniques and methods have been tested in order to simulate flooding and runoff. An important parameter the "Manning roughness coefficient" was integrated in these methods, which comprises a flow resistant factor and a function of land cover in flooded areas (De Roo 1999). A segmentation and classification approach of IKONOS-2 imagery (Van der Sande et al. 2003) aims to produce detailed land cover maps for flood damage assessment as well as detailed maps of roughness coefficients for flood simulation models. The fuzzy mathematical models are introduced in the field order to improve probability estimation and evaluation of flood risk with incomplete data sets (Qiong et al. 2012; Pourghasemi et al. 2012). However, these different techniques and methods lack comparison between parameters in order to obtain the most accurate results and give weights close to reality.

In this study, the aim was to identify flood-susceptible areas in order to find solutions for the assessment and management of floods and to determine which region deserves the most engagement in the development of risk diminution measures or mitigation procedures. Flood mapping and risk analysis of different regions need the use of multiple factors (Poussin et al. 2014). As a result, multicriteria decision analysis (MCDA) methods have been successfully used in various researches and have been recognized as an important tool for analyzing complex decision problems. MCDA integrate a large number of criteria such as technical, environmental, and socioeconomic factors (Liu et al. 2003) to achieve a perfect decision (Ghanbarpour et al. 2013). This process is established using the existing conditions as a reference to identify flood hazards areas (Yang et al. 2011). Coupled to the Geographical Information System (GIS), the MCDA was used for mapping inundation zones. Indeed, the GIS techniques facilitate treatment and analysis of the spatial data and make easy the visualization, interpretation, and evaluation of the MCDA results (Wang et al. 2011). Eight spatial parameters have been used in this study: Land use-Land cover, drainage density, rainfall, lithology, elevation, slope, soil and groundwater level.

Analytical hierarchy process (AHP) has been developed by Saaty in 1980 and it is considered a mathematical technique of multi-criteria decision-making (Matori et al. 2014). AHP technique has been applied to flood susceptibility mapping and has proved its effectiveness, especially in groundwater mapping (Kaliraj et al. 2014; Razandi et al. 2015), landslide susceptibility mapping (Althuwaynee et al. 2014), and in chemical fields (Hanratty and Joseph 1992; Pirdashti et al. 2009).

This technique evaluates the importance of factors, according to weight values. After, the weight determination, the Flood Hazard Index (FHI) can be computed and used to assess the rate of the flooding probability (Elkhrachy 2015). Hazard Index Sensitivity (FHIS) is identified to examine the sensitivity pairwise comparison method against the changes in criteria weights. Consequently, we noticed that the FHIS is efficient in situations as where uncertainty exists in the definition of the importance of each factor (Yahaya 2008).

The new approach proposed in this study is applied for the first time in the region. It allows us to compare between the parameters, and test and classify them according to their intervention in the production of the flood in the studied zone. This proposed approach is applicable in various zones. The scientific results which are derived from this work can assist planners, engineers, and governments to perform proper actions in order to prevent and mitigate the flood occurrence in the future.

Material and methods

Study area

The study area is located in the North-East of Tunisia (Fig. 1a), North Africa, between 10° 1′ 0″ E to 10° 20′ 30″ E longitude and from 36° 45′ 0″ N to 36° 58′ 0″ N latitude, overlooking the Mediterranean Sea in the East. It extends from Morneg in the South to the Djebel Ammar (328 m) and Ennahli (201 m) anticlines in the North, and it is bounded by the Djebel Sidi Salah and Djebel Ain El Krima anticlines in the West (Fig. 1b). The surface which is concerned by this study is about 524.4 km^2 including two sebkhas, that of Ariana (50 km^2) and Séjoumi (30 km^2) and it even integrates the Lake of Tunis (40 km^2). Ariana, Soukra, and Manouba plains, surrounds these humid fields. The Tunis sector is characterized by a semi-arid climate (Emberger 1955) with a hot winter of an annual mean precipitation of 469.5 mm, recorded at five meteorological stations from 1985 to 2015 (DGRE 2015, CRDA 2015). The mean monthly rainfall distribution has shown that the rainiest period extends from October to March, with a maximum mean monthly value in December (77 mm). The driest months of the year are June, July, and August with a minimum recorded in July (3.2 mm).
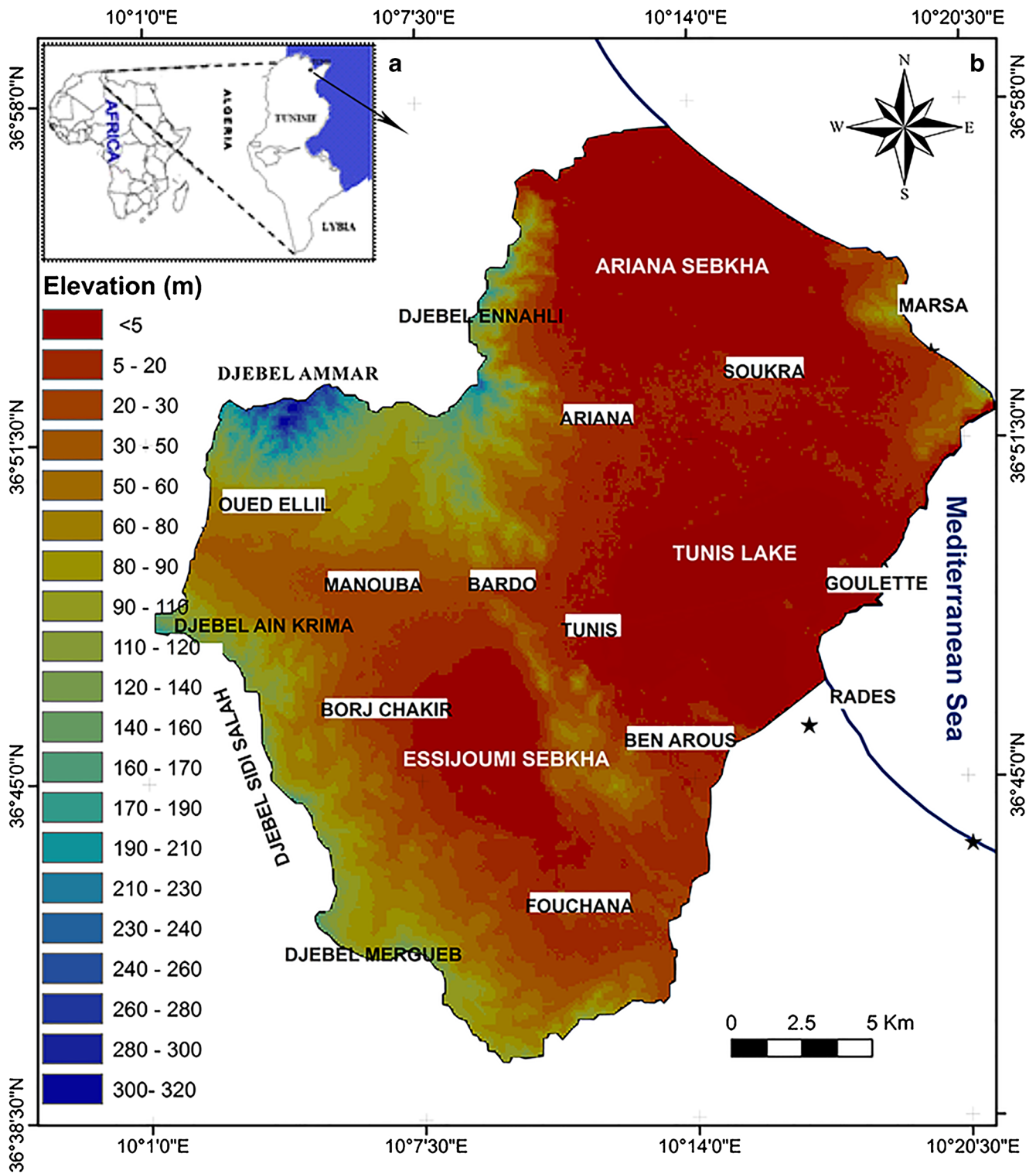
Fig. 1 **a** Location of Tunisia. **b** Location of the study area

The mean of monthly temperature reaches its maximum (34.5 °C) in August and its minimum (7.7 °C) in January. Monthly inter-annual wind variability ranges from 20 to 27.8 km/h (INM 2015). The mean annual precipitation for the period 1985–2015 is about 469.5 mm, which corresponds to the mean annual rainfall water volume of 246.3×10^6 m³. Potential evapotranspiration has been computed using the Thornthwaite method (Thornthwaite and Mather 1957). The real evapotranspiration (ETR) is about 1097.76 mm and the potential evapotranspiration (ETP) is about 41.9 mm/years.

Hydrographical network covering the study area is composed of permanent and impermanent streams. There are three major rivers discharge to the Essijoumi Sebkha (Gueriana, Bardo, El Meleh) and two rivers (Guereb and Roriche) discharge to the Tunis Lake. The geological formations outcropping in the study area are composed of Triassic, Cretaceous, Paleogene, Neogene, and Quaternary series. The Triassic is exposed at jebel Ammar and Jebel Mergueb. It is composed mainly of gypsum, gypsum clay, marl, and dolomite (Boutib 1998). The high structures (Djebel Ammar 328 m, Djebel Ennahli 201 m) are covered essentially by limestone or marl-limestone alternation from Jurassic to Eocene ages (Pini 1971; Pini and Kchouk 1971). The hills are composed mainly of sandstone, clay, and sand of Olig-Pliocene (Bujakka et al. 1971). The continental Mio-Pliocene series lay unconformably on the Oligocene deposits (Ben Ayed et al. 1979; Boutib 1998). The Miocene is characterized by sandstone, sand, and sandy clays (Lajmi 1968). The Pliocene strata expose mainly at Djebel Ain El Krima and Ariana-Belvédére where they are represented by fluvial-deltaic sediments (Boutib 1998).

Finally, the Quaternary deposits cover the greater part of the study area, usually composed of silt, conglomerate, clay, silt, and sandy limestone accumulation (Oueslati 1994). The phreatic aquifer of the sector is mainly formed during the Plio-Quaternary. Rainwater directly infiltrates into the soil, recharging the aquifer (DHU 2015). In the major part of the area, the water table depth is about 6 m while it is relatively deep (greater than 10 m) in a small area around the hills and Djebels. The transmissivity varies between 3.10^{-3} and 5.10^{-3} m^2/s.

In the arid and semi-arid regions, especially in the rapidly expanding towns and cities, intense urbanization has led to a high demand of groundwater resources (Farah et al. 1997; Murthy 2000) (Table 1). Consequently, the groundwater quality has been degraded (Fritch et al. 2000). There are various sources of groundwater pollution such as discharge of untreated sewage in water courses. It is the most important source of pollution of both surface and groundwater (Naik et al. 2008).

The Tunis region has been undergoing an intense population growth. It increased by 814,853 thousand people between 1994 and 2014 (INS 2015) (Table 2). Results increased the demand for housing and new residences (Givisiez and Oliveira 2009), urban expansion, and industrial centralization (Chabbi and Abid 2008). Fast, visible, and critical changes in land use and settlement have

Table 1 Resources and exploitation of ground water (DGRE 2015)

Years	Resources (Mm^3/an)	Exploitation (Mm^3/an)	Salinity (g/l)
1990	18.9	7	1 to 5
1995	17.9	7	1 to5
2000	17.9	4	1 to 5
2005	20.87	9.35	0.5 to 10
2010	18.85	9.2	0.5 to 10
2015	18.72	8.73	0.5 to 10

Table 2 Population growing (INS 2015)

Years	1994	2004	2014
Population (thousands)	1,828,842	2,247,792	2,643,695
Accomodations	399,808	593,015	820,227

been taking place at a remarkable, reshaping the landscape and affecting the environment (Weng 2001). Waterproofing rate of the soil (IMP) varies between 10 and 90% (DHU 2015). More than half of the Tunis sector watershed has been altered by human activities. A natural flow of rainwater is seriously prevented, because the rain that would normally seep into the soil has to flow across construction surfaces and through storm-water pipes, increasing the volume and velocity of runoff (Tucci et al. 1995) causing environmental risks, such as flood hazard.

Methodology

The methodology adopted in the current study is summarized in the diagram of the Fig. 2. The main goal of this study is to define flood-susceptible areas by using the GIS environment (Forte et al. 2006), SRTM (Shuttle Radar Topography Mission), and Remote sensing data (Brivio et al. 2010). The second objective is to calculate Flood Hazard Index (FHI) by incorporating multiple criteria decision-making (MCDM) (Drobne and Lisec 2009) and analytical hierarchy process (AHP) (Generino et al. 2014).

Initially, various data sources were used and introduced in ArcGIS including satellite images, time series observations, spatial data, and geological and topographic maps. However, a selected set of parameters were integrated into the present study according to their significant role in flood area selection. Only eight thematic layers were approved for the inundation zoning including drainage density, land use/land cover, rainfall, slope, soil type, elevation, lithology, and groundwater level.

The slope map of the study area was deduced directly from DEM (digital elevation model) data extracted by SRTM global 1 arcsecond (30 m). The slope percentage values were estimated by the spatial analysis tool in Arc-info-GIS 9.3. SRTM was further utilized to develop the elevation map of the area using ArcGIS software. The drainage density network was created using the line density analysis Tool in ArcGIS.

The piezometric map of the year 2015 was estimated by the GIS model kriging tool. It allows, as a result, the groundwater level surface to be defined at ungauged locations from local information. The annual mean rainfall was calculated using monthly rainfall data collected from the General Department of Water Resources (DGRE) of Tunisia in five rain gauges for 30 years from 1985 to 2015. Subsequently, an annual mean rainfall map was generated and saved as a layer in ArcGIS platform. Either the soil map taken from the General Department of Water Resources was georeferenced and digitized as a layer in ArcGIS. Lithological map was produced by assembling the four
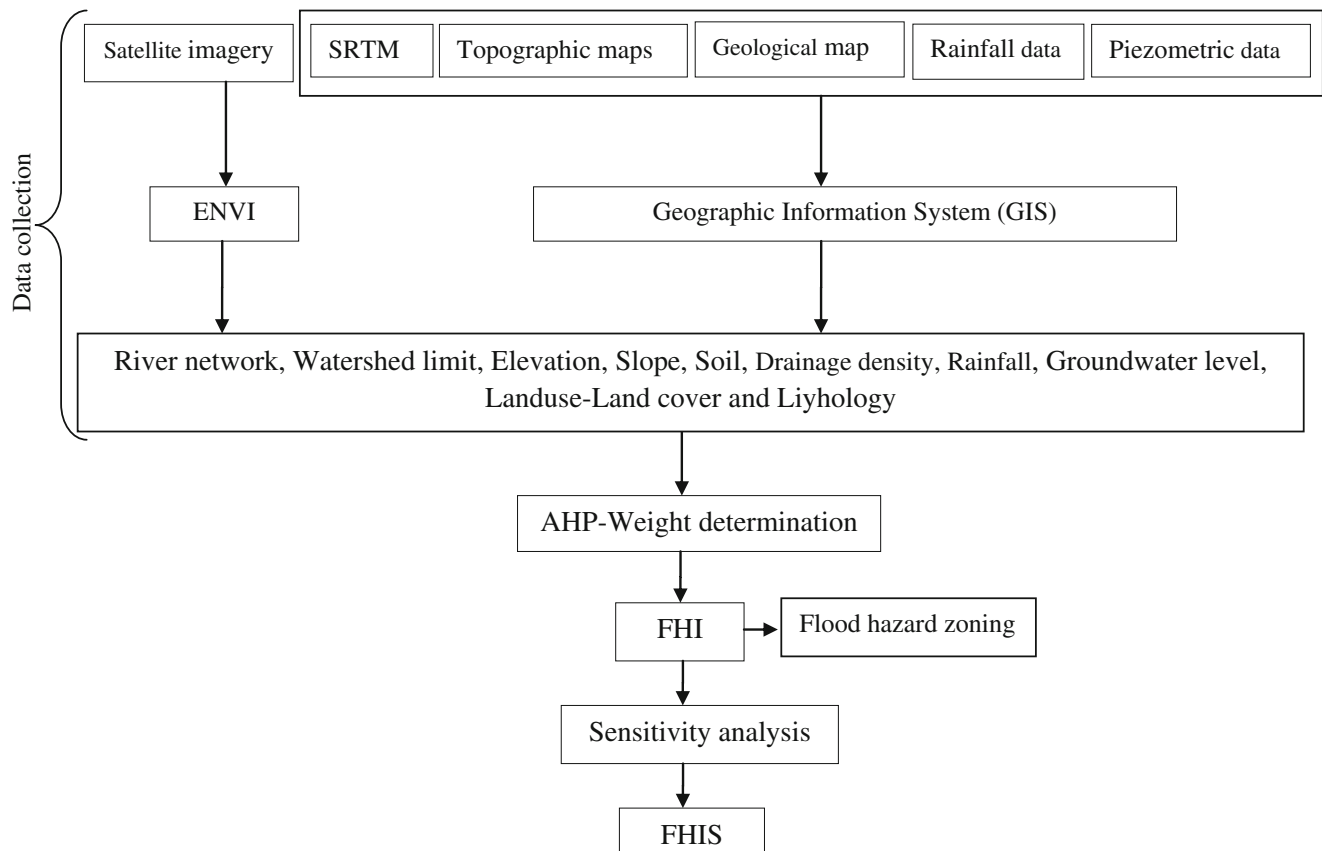
Fig. 2 Conceptual model based on multi-criteria decision analysis (MCDA) and analytical hierarchy process (AHP) for flood susceptibility mapping by GIS

geological maps of Tunis, La Goulette, La Marsa, and Ariana sectors on a 1/50000 scale. Afterwards, land use/land cover map was obtained by the treatment of satellite images from Landsat 8 Sensor on a scale of 1/500000 using ENVI model and converted into raster format (30 m resolution) legible by ArcGIS.

The factors used to assess the flood-susceptible areas do not have the same degree of influence. Evaluating the effect of each factor alone does not provide the complete required picture. The integration of all factors together was necessary. Indeed, the influence of factors on each other is determined using a schematic sketch according to Shaban et al. (2001). This method allows to determine the weight of each factor on all other factors. One (1) point is assigned to a major effect and half point (0.5) to a minor effect. Next, the rate factor is calculated as the summation of the points attributed to the effects of the factor (Shaban et al. 2006).

To conduct a comprehensive assessment of the influence of each factor on flood generation in the study area, a weight value equivalent to its relative importance was assigned to each factor. This weight was determined by pairwise comparison process proposed by Saaty in 1980.

The first stage of the AHP technique consists to define of the decision problem. Preparing a pairwise comparison matrix constitutes the second stage of the technique (Yaralıoğlu 2004). An n*n dimensional pairwise comparison matrix of the conditioning factors is prepared at this stage. The importance value scale

proposed by Saaty (1980) is respected (Table 3). In this stage, every factor was given an arithmetic value between 1 and 9, depending on its significance compared to the other factor which is coupled to it. An arithmetic value of 1 means that both factors are equally significant. However, a value of 9 indicates that a row factor is much more significant than the corresponding column factor which it has been compared to Saaty 1980.

The proposed methodology suggests a pairwise comparison, using an 8×8 matrix. Afterwards, a numerical index named consistency ratio (CR) was used to examine the consistency pairwise comparison matrix (Table 4).

Table 3 Saaty scale (1980)

Scale	Numerical rating	Reciprocal
Extremely importance	9	1/9
Very to extremely strongly importance	8	1/8
Very strongly importance	7	1/7
Strongly to very strongly importance	6	1/6
Strongly importance	5	1/5
Moderately to strongly importance	4	1/4
Moderately importance	3	1/3
Equally to moderately importance	2	1/2
Equally importance	1	1

Table 4 Random inconsistency indices

n	3	4	5	6	7	8	9	10
RI	0.58	0.9	1.12	1.24	1.32	1.41	1.45	1.49

In Table 5, the criteria selected are sorted in a hierarchical manner. The values of each row characterize the importance between two parameters. The first row of the table illustrates the importance of land use-land cover in regard to the other parameters which are placed in the columns. For example, land use-land cover is significantly more important from the groundwater level, and therefore assigned the value 9. Land use-land cover has been considered as the most important parameter since flooded areas are often located in urban zones. These weights were normalized according the method of the AHP. The model was integrated into a GIS system in order to realize a flood hazard map (Stefanidis and Stathis 2012).

Afterwards, the consistency ratio (CR) was determined. If CR ratio is superior to 0.1 the judgments may be too inconsistent to be reliable. However, when CR is equal to 0, the judgments seem to be absolutely consistent (Elkhrachy 2015). To calculate the value of (CR), the consistency index (CI) is divided by the random index (RI) Eq. (1). The RI is dependent on the number of criteria (Kazakis et al. 2015).

$$CR = CI/RI \tag{1}$$

Where CI is the consistency index, and RI is the random inconsistency indices.

$$CI = (\lambda - n)/(n - 1)$$

n   number of factors and λ: average value of the consistency vector.

Table 5 A matrix of pairwise comparisons of eight criteria for AHP process

	LULC	EL	LI	RF	DD	SP	SL	GL	SUM
LULC	1.00	1.29	1.29	1.5	2.25	3	4.5	9	23.82
EL	0.78	1.00	1.00	1.17	1.75	2.33	3.5	7	18.53
LI	0.78	1.00	1.00	1.17	1.75	2.33	3.5	7	18.53
RF	0.67	0.86	0.86	1.00	1.50	2.00	3	6	15.88
DD	0.44	0.57	0.57	0.67	1.00	1.33	2	4	10.59
SP	0.33	0.43	0.43	1.00	0.75	1.00	1.5	3	8.44
SL	0.22	0.29	0.29	0.33	0.50	0.67	1	2	5.29
GL	0.11	0.14	0.14	0.17	0.25	0.33	0.5	1	2.65

LULC land use-land cover, *EL* elevation, *LI* lithology, *RF* rainfall, *DD* drainage density, *SP* slope, *SL* soil, *GL* ground water level

In the present case of study, the eight factors used for hazard area mapping are examined separately. We also divided each factor into a number of classes and gave a weight for every class. The maximum and minimum weights for each class of every factor vary respectively from 1 to 10. Next, the weights assigned to different classes of the individual criterion and their normalized weights are calculated. The class weights used are related to the effect of each class to the flood hazard. All factors use the same classification; however, they do not contribute to the same amplitude (Stefanidis and Stathis 2012).

First, the information collected from different data sources is processed in the GIS. Then, the FHI is calculated by the following expression Eq. (2) to evaluate the flooding probability rate (Elkhrachy 2015):

$$FHI = \sum_{i=1}^{n} Wi\,Ri \tag{2}$$

Where Ri is the rating of the factors, Wi is the weight of each factors, and n correspond to the number of the parameters.

Therefore, Eq. (2) is written in the next form:

$$FHI = W_{LULC}\,R_{LULC} + W_{EL}\,R_{EL} + W_{LI}\,R_{LI} + W_{RF}\,R_{RF}$$
$$+ W_{DD}R_{DD} + W_{SP}\,R_{SP} + W_{SL}R_{SL} + W_{GL}R_{GL}$$

At the end, single parameter sensitivity analysis is determined to assess the impact of each parameter on the vulnerability index. This test of sensitivity is produced because the numerical values attributed to these parameters are arbitrary (Zghibi et al. 2016). The initial arbitrary weights by AHP are replaced with effective weights (Kazakis et al. 2015; Stefanidis and Stathis 2012), and calculated according to the next equation Eq. (3):

$$W = [(P_r * P_w)/V] * 100 \tag{3}$$

Where W is the effective weight of each parameter, P_r is the parameter's rating, P_w the parameter's weight, and V is the aggregated value of the applied index.

The effective weights are then employed to calculate the revised Flood Hazard Index (FHIS) by the sensitivity analysis method. For the evaluation of flood risk-prone areas, the parameters' classes of each factor selected should be adjusted to the local characteristics of each study area.

Results and discussion

Multi-influencing factors of flood Hazard zones

Slope map

Topography has a main effect on flood production and redistribution. The slope percent is an indicator surface to define

the flood sensitivity (Youssef et al. 2011). An area with a low slope has a higher risk because it is easily to be submerged by flood. On the other hand, a surface with a high slope is less exposed to flood risk, because these floods can be rapidly drained to down slope (Chen et al. 2015). Therefore, this factor plays an important role in determining the amount of surface runoff and infiltration, and thus affecting flood sensibility (Rahmati et al. 2016a, b). Based on the slope, the study area can be divided into five slope classes (Fig. 3a). This weight of each class (betwen 1 at 10) is according to its intervention in the generation of the flood. The weight 10 is attributed to the first category (0 to 2%), composed by the nearly flat terrain highly exposed to the inundation. This range represents about 54.4% of the study area.

Elevation map

The altitude has significant impact on the propagation of flooding in the study area. In addition, this parameter has an important role in the control of the followed direction movement and in the depth of the flood. The resulting map was grouped into five classes showed in Fig. 3b.

Rainfall map

Averages of annual rainfall were calculated according to monthly rainfall data from five rain gauges. We used the data for 30 years between 1985 and 2015, where the mean annual precipitation is around 469.5 mm. Subsequently, a mean annual rainfall map was generated by employing interpolation techniques of kriging used by ArcGIS software (Fig. 4a). Precipitation scale was divided into 4 classes from 440 to 520 mm. The first class represents values under 460 mm (6.62%), the second one represents values between 460 and 480 mm (77.27%), the third one represents values between 480 and 500 mm (12.5%), and the fourth one represents values over 500 mm (3.59%). A weight of 2 is proposed to characterize the lowest precipitation interval and a weight of 10 is attributed to the highest level range.

Lithological map

The fourth significant parameter used to define the flood zone is lithology (Svoboda 1991). This factor is related to the permeability and the capacity of water storage that vary according to rock types (Oikonomidis et al. 2015). When the rock is impermeable, the rainfall water infiltration is less important, which favors extension of runoff surfaces and amplify flood event effects (Kourgialas and Karatzas 2011). The lithology map of the study area was produced by an analysis in a GIS environment of the geological maps of Tunis sector that were prepared at the 1:50000 scale by the Topography and Cartography Office (OTC 1980) in Tunisia. The study area was covered by various types of lithological formations extending from the Triassic to the Quaternary (Bujakka et al. 1971; Maamri and Ben Salem 2000) (Fig. 4b).
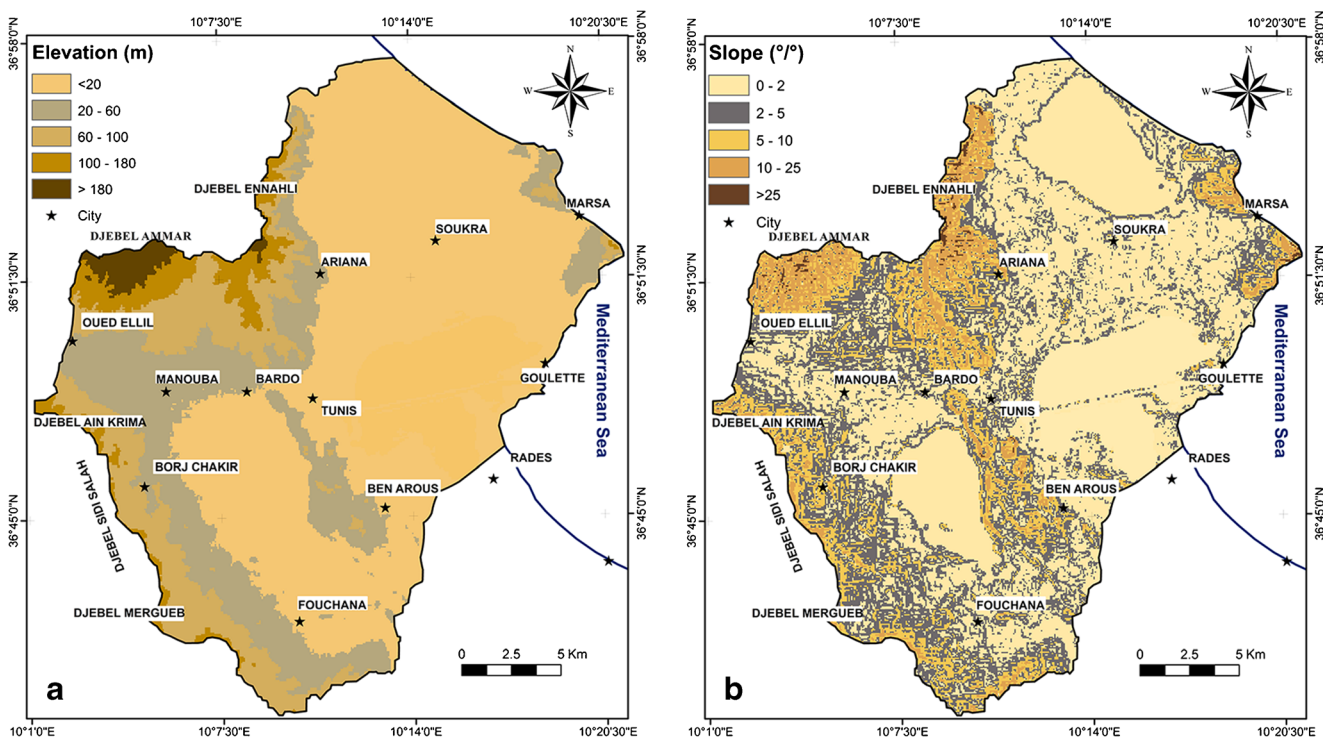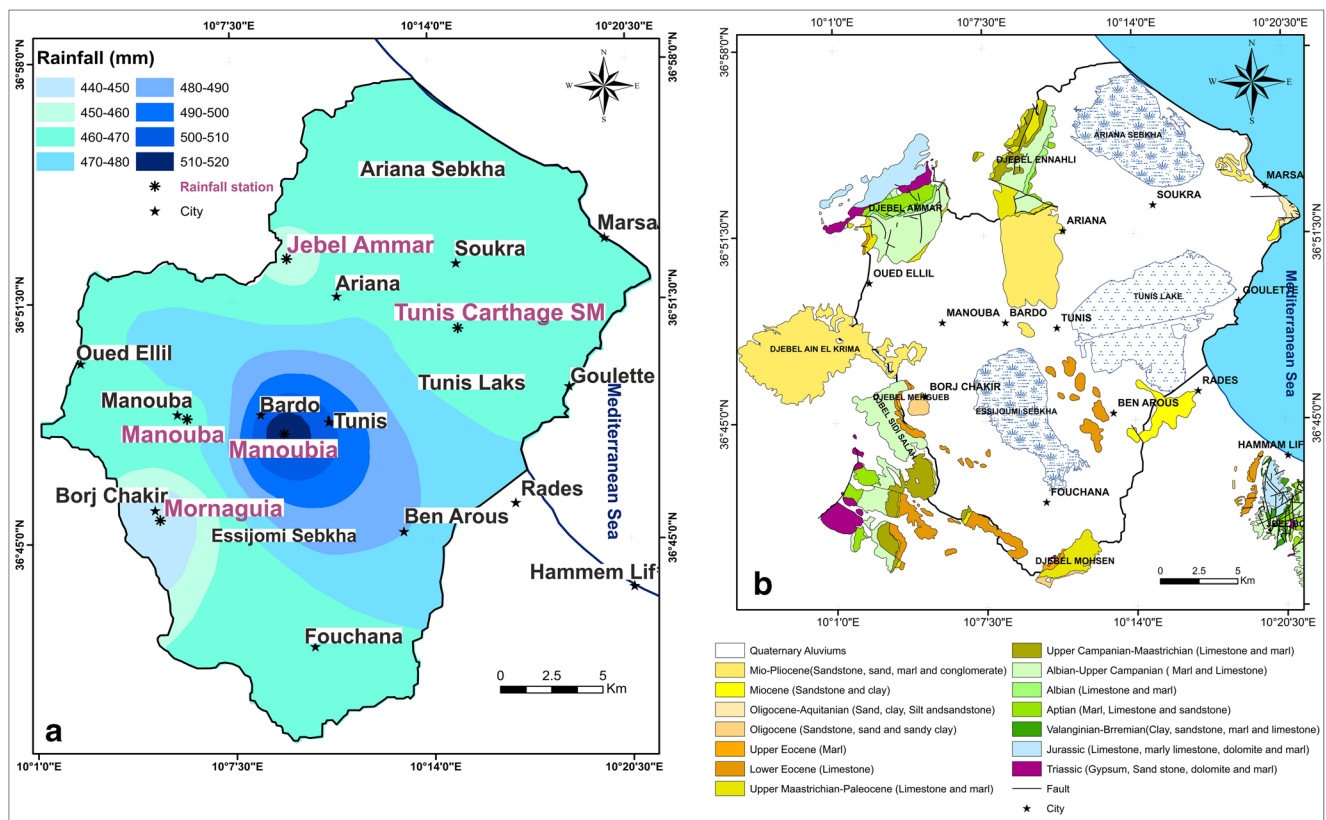

Fig. 3 a Slope. b Elevation

Fig. 4 a Rainfall. **b** Lithology

Land use/land cover map

Land use/land cover constitute the principal factor to identify areas, which are susceptible to be submerged by flooding (Nuissl et al. 2009). Land use influences infiltration rate. For example, forest and vegetation favor water infiltration (Kourgialas and Karatzas 2011). On the other hand, urban area, which is mostly made from impermeable surfaces and bare lands, increase the storm runoff (Tehrany et al. 2014). These land use-land cover classes are determined from the satellite images. Therefore, we obtained the five classes of the land cover, such as urban areas, forest, irrigated land, crop land, and bare soil. A considerable surface of the studied area is urbanized (51, 5%) (Fig. 5a).

Soil map

In the current study, the thematic soil type map was displayed in a GIS layer that ranked soils based on their textures and structures. Effectively, the texture and structure of each soil type can influence significantly their permeability and consequently their capacity of water storage. Thus, we assigned the lowest weight value (2) to sand class and the highest one (10) to the soil type corresponding to urban areas (Senanayake et al. 2016) (Fig. 5b).

Groundwater level map

In fact, during floods, a rapid change in groundwater outflow was observed due to the new infiltrated water during heavy rainfall. This water flow coming in a brief time range can obviously increase the groundwater level and affects the soil infiltration capacity (Troch et al. 1993). In this way, it increases the hydraulic pressure in the aquifer and in areas where groundwater is very near to surface (Upton and Jackson 2011). The depth of the groundwater level was measured all over the piezometric network and the spatial interpolation of these piezometric values for different time scale allows a mapmaking of groundwater level surface to be constructed using GIS software. The GIS is one of the most appropriate softwares for contouring groundwater level data, which is generally a non-stationary variable (Gundogdu and Guney 2007). The depth of the water table was prepared by considering the highest elevations of the static water levels (2015). The resulting map was classified into five classes and areas underlined by shallow depth (0–2 m depth) were considered as the most vulnerable to the risk of flooding (Fig. 6a). Nevertheless, the water table depth in the Tunis sector is lower than this value and varies between 0 and 32 m above sea level, decreasing gradually from the West to the East. According to the water-table depth, 70% of the Tunis region is characterized by a very high to moderate flood
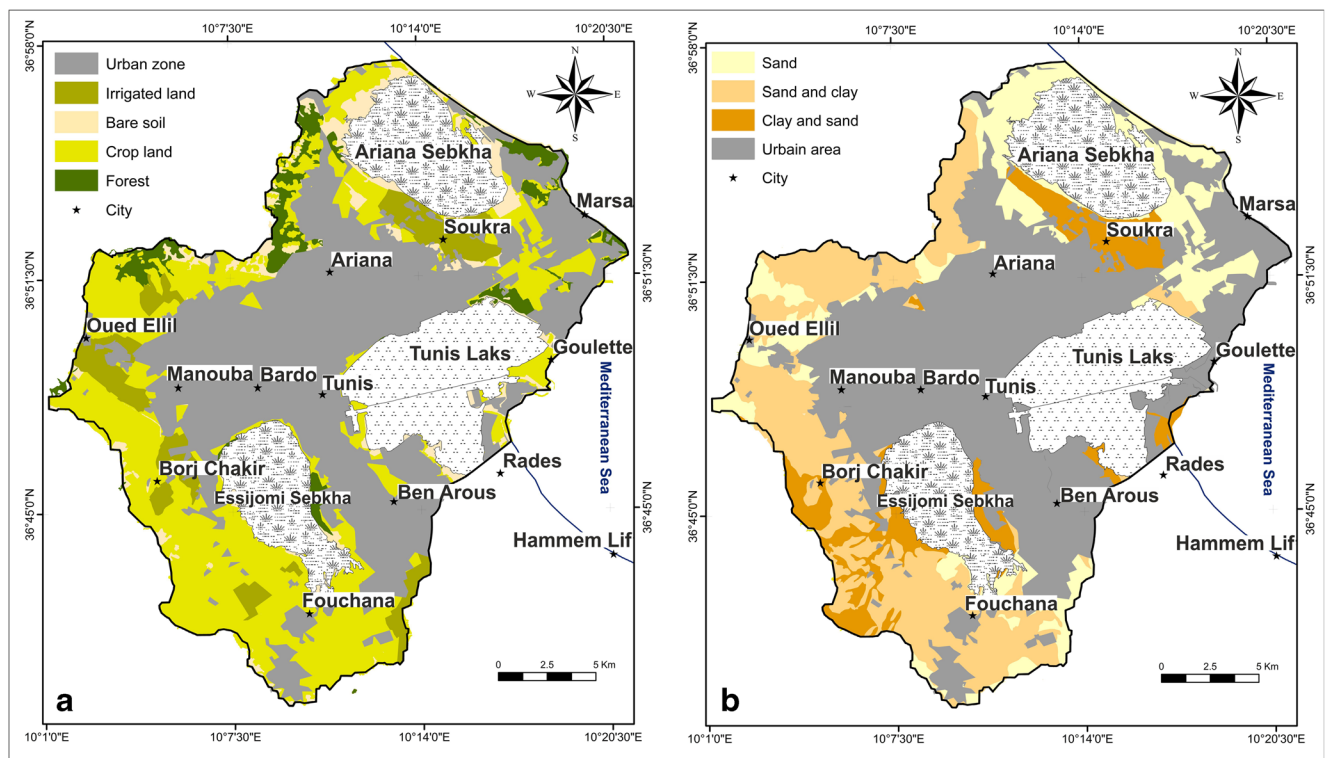
Fig. 5 **a** Land use-land cover. **b** Soil

susceptibility. The less susceptible sites (> 8 m) with ratings 1 and 2 represent nearly 30% of the total area. However, the most sensitive sites with ratings 8 and 10 are located in the center part and near the coast.

Drainage density map

Drainage density is an important element of flood control measures (Ogden et al. 2011), which expresses the length of rivers per unit of area (Km/km^2) (Magesh et al. 2012). The drainage density map was produced employing the line density analysis tool in the Arc GIS environment. After that, a reclassification into four classes (from low to high), according to the class boundaries of Table 6, has been conducted. High drainage density (1.5 to 1.9 Km) was recorded in the relief of the study area. On the other hand, the low drainage density (0– 0.5 km) is recorded on the plains (Fig. 6b). The raster drainage network density file was assigned a weight of 6% (0.06) in the calculation of the flood susceptibility final map and according to AHP methodology.

Interrelationship and pairwise comparisons of the factors

Multi-influencing factors of flood-susceptible areas

The eight influencing factors, established in the preceding section, were used to estimate the flood sensitive areas

and generate the corresponding map, such as lithology, slope, elevation, land use-land cover, drainage density, soil type, rainfall, and groundwater level. The dangerous zones cannot be estimated by considering the effect of each factor separately, since all factors do not have the same degree of influence in the hazardous areas (Kazakis et al. 2015). The factors weights were given by applying the relation determined by Shaban et al. (2001), which take into account the influence of each factor on all other factors. A continuous line between two factors indicates that one factor has a major and principal effect on the other pointed by the arrow. A discontinuous line between two factors indicates that one factor has a minor and indirect effect on the factor pointed by the arrow (Fig. 7).

To quantify the two types of effects, one (1) point is attributed to a major effect and half a point (0.5) to a minor one (Shaban et al. 2006). Next, the rate factor is calculated as the summation of the points attributed to the effects of the factor (Shaban et al. 2006). According to this relation, the rate weight of the land use-land cover factor is significantly higher than the groundwater level.

Relative weights of criteria

A pairwise comparison is shown in Table 5, using an 8 × 8 matrix, where diagonal elements are equal to 1. The first row of the table illustrates the importance of land use/land cover in
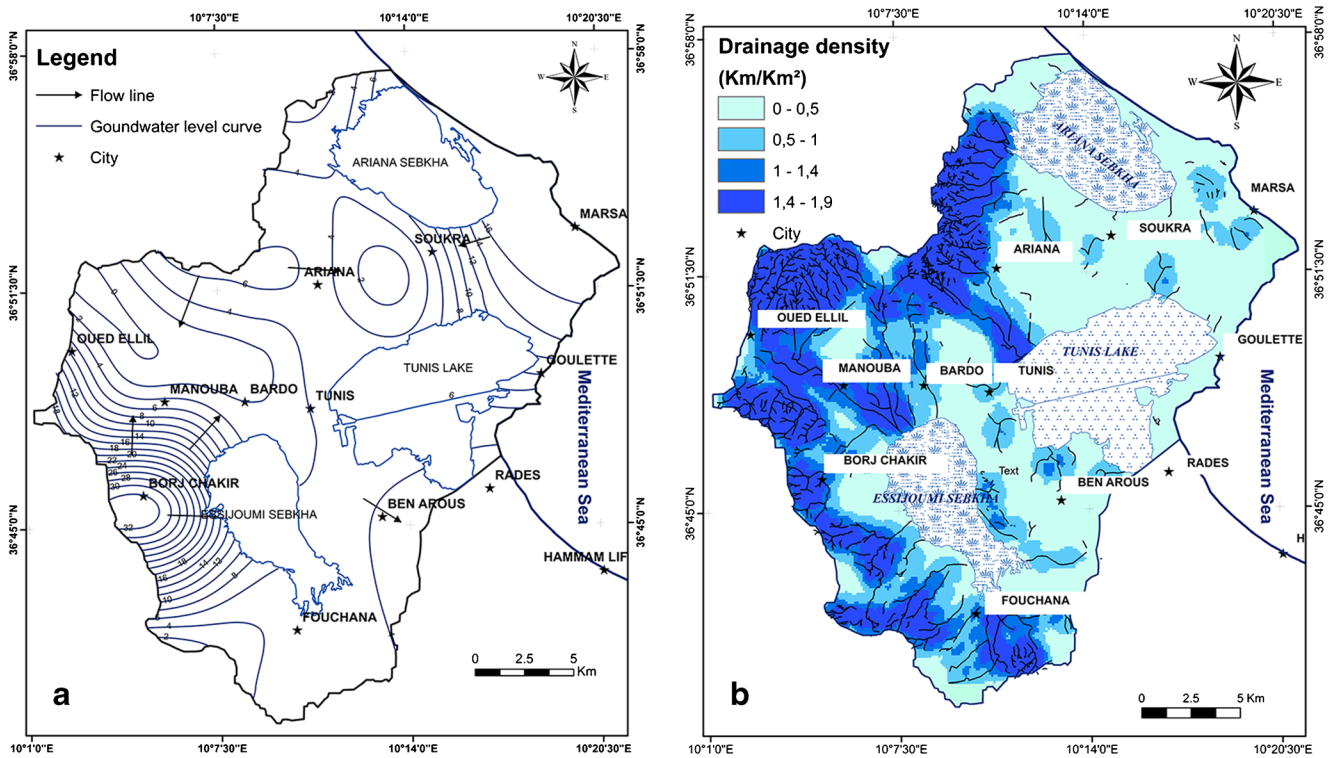
Fig. 6 **a** Groundwater level. **b** Drainage density

regard to the other parameters which are placed in the columns. Since our basin containing urban areas, land use/land cover has a higher influence in flood occurrence compared to the other factors. Land use/land cover is significantly more important than groundwater level, and therefore assigned the value 9. On the first hand, elevation and lithology are considered less important than land use/land cover. On the other hand, they are considered more important than rainfall, drainage density, slope, and soil-type factors. Although, all these parameters were prioritized in other previous studies.

Determined consistency ratio (CR)

RI is dependent on the number of criteria (Matori et al. 2014) (Table 4). In this study, the criteria are eight and the result RI = 1.41.

Finally, the consistency ratio has been calculated CR = 0.013 (Eq. 4), since CR value is inferior than 0.1 and the weights consistency are accepted.

$$CR = CI/RI \qquad (4)$$

CI   Consistency index and RI = Random inconsistency indices.
CI $(\lambda - n) / (n - 1)$
n   number of factors and λ: average value of the consistency vector.

λ 8,13
CI   0,019
CR   0,013 < 0,1

Classes of the factors and according weights

The contribution of each class to the hazardous areas expressed by a percentage is demonstrated in the last column of Table 6. The percentage of each class was computed as the ratio of the total factor weight to the grand total. Based on the results, the weight of the urban area is significantly higher than the other class of land use-land cover factor (bare soil, irrigated land, crop land, and forest).

Flood Hazard Index (FHI)

The FHI is found to evaluate the rate of flooding probability (Elkhrachy 2015), which was calculated by the following equation:

$$FHI = 0.23\, R_{LULC} + 0.18\, R_{EL} + 0.18\, R_{LI} + 0.15\, R_{RF}$$
$$+ 0.10 R_{DD} + 0.08\, R_{SP} + 0.05\, R_{SL} + 0.03\, R_{GL}$$

Flood susceptibility map

The eight maps that were developed after the weighting method and AHP were combined and superposed in the (GIS)

**Table 6** Classes of the factors and according weights

Factors	Class	Rate	Factor weight	Class weight	Weight (°/°)
Land use/land cover	Urban area	10		2.3	38
	Bare soil	8		1.84	31
	Irrigated land	5	0.23	1.15	19
	Crop land	2		0.46	8
	Forest	1		0.23	4
Elevation	< 20	10		1.8	38
	20–60	8		1.44	31
	60–100	5	0.18	0.9	19
	100–180	2		0.36	8
	> 180	1		0.18	4
Lithology	Marly limestone	10		1.8	40
	Silty Clay	8	0.18	1.44	32
	Sand and clay	6		1.08	24
	Alluvium quaternary sediments	1		0.18	4
Rainfall	500–520	10		1.5	38
	480–500	8	0.15	1.2	31
	460–480	6		0.9	23
	440–460	2		0.3	8
Drainage density	1.4–1.9	10		1	38
	1–1.4	8	0.1	0.8	31
	0.5–1	6		0.6	23
	0–0.5	2		0.2	8
Slope	0–2	10		0.8	38
	2–5	8		0.64	31
	5–10	5	0.08	0.4	19
	10–25	2		0.16	8
	> 25	1		0.08	4
Soil	Urban area	10		0.5	38
	Clay and sand	8	0.05	0.4	31
	Sand and clay	6		0.3	23
	Sand	2		0.1	8
Groundwater level	0–2	10		0.3	38
	2–4	8		0.24	31
	4–8	5	0.03	0.15	19
	8–10	2		0.06	8
	> 10	1		0.03	4

environment. The flood susceptibility map supports the identification of inundation sensitive areas, while records of historical flood events verify the accuracy of the methodology.

The final map of the flood sensitivity area was constructed and classified into five major classes with flood potentiality from very low to very high. Respectively, we find that 2.85% of the study area represents the very low class, 7.5% of the area represents the low class, 17.95% of the area represents the moderate class, 20.63% of the area represents the high class, and 51.06% of the area represents the very high class (Fig. 8). It appears that areas of

very high potentiality occupy a surface of 270.37 km², which covers the largest part of the study region. Historically, this region has suffered from several floods (on 1989, the Gulf of Tunis, 2003 the Tunis sector, October 2007 the area of Sabbalet Ben Ammar of the region of Ariana and in 2017, the Manouba region).

Obviously, we can observe the coincidence between the zones of the highest flooding risk and the urban areas. This index accordingly received a higher weight. However, this effect is especially critical to inundation and produces relatively a significant impact on the
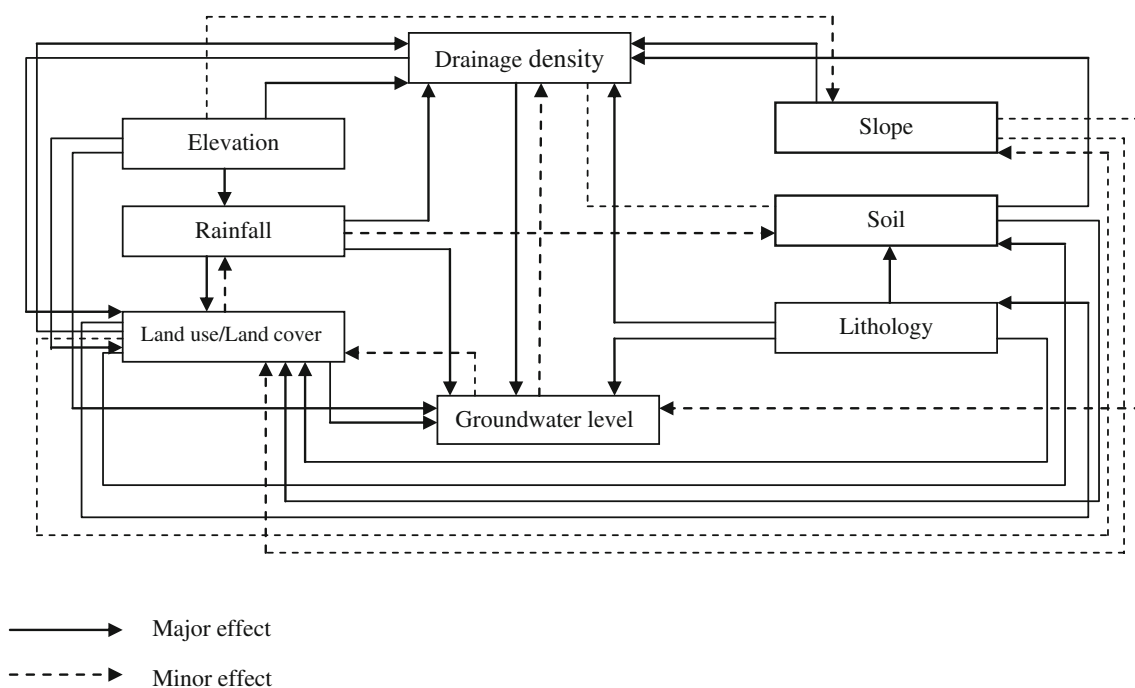
Fig. 7 Interrelationship between that multi-influencing factor concerning the flood-susceptible areas

resultant flood susceptibility map. It is also interesting to notice that three criteria, land use/land cover, elevation, and lithology (Figs. 5a, 3b, and 4b), received high weights which can be obviously observed, particularly in the Northeast, south-east, and central area. However, the influence of other criteria (rainfall, drainage density, slope, soil, and groundwater level) are not visible. These criteria are assigned to the smallest weights and do not have a significant impact on the inundation phenomenon. Therefore, these results provide a baseline information, which needs to be considered during flood management.

Sensitivity analysis FHIS

Single parameter sensitivity was developed to evaluate the impact of each parameter on the flood hazard index. This sensitivity test type is produced because the numerical values attributed to these parameters are essentially arbitrary (Al-Adamat et al. 2003; Zghibi et al. 2016). In terms of sensitivity analysis, the initial arbitrary weights given by the theoretical method (AHP) are replaced with "effective weights" (Kazakis et al. 2015) and calculated according to the following equation:

$$W = [(P_r * P_w)/V] * 100 \qquad (5)$$

Where:

W   the effective weight of each parameter, P_r: the parameter's rating, P_w: the parameter's weight and V: the aggregated value of the calculated index.

$$FHIS = 0.3\ R_{LULC} + 0.21\ R_{EL} + 0.18\ R_{LI} + 0.14\ R_{RF}$$
$$+ 0.07\ R_{DD} + 0.04\ R_{SP} + 0.05\ R_{SL} + 0.02\ R_{GL}$$

The effective weights are then used to calculate the revised Flood Hazard Index of the sensitivity analysis (FHIS) (Akbari and Rahimi Shahrbabaki 2011). The FHIS analyze the same parameters signed previously in studied and classified by the FHI, but with different weights (the average effective weight of the sensitivity analysis). FHIS estimated in a range of different values of the criteria and its comparison with the FHI shows the dependence and sensitivity of flood on the parameters selected. For the assessment of flood hazard areas, the parameters classes of each factors selected should be adjusted to the local characteristics of each study area (Kazakis et al. 2015).

Table 7 shows the effective weight presented by the sensitivity analysis and the theoretical weight attributed by the AHP method. The sensitivity analysis concluded that land use-land cover, elevation, rainfall, and lithology have a bigger influence in the studied region. The effective weight of the rainfall, drainage density, slope, and groundwater level (14%, 7%, 4%, and 2% respectively) represented low effective weight compared to their theoretical weight (15%, 10%, 8%, and 3% respectively).

Conclusion

Inundation is natural risk that impacts the populations and structures within the affected areas. The research proposes
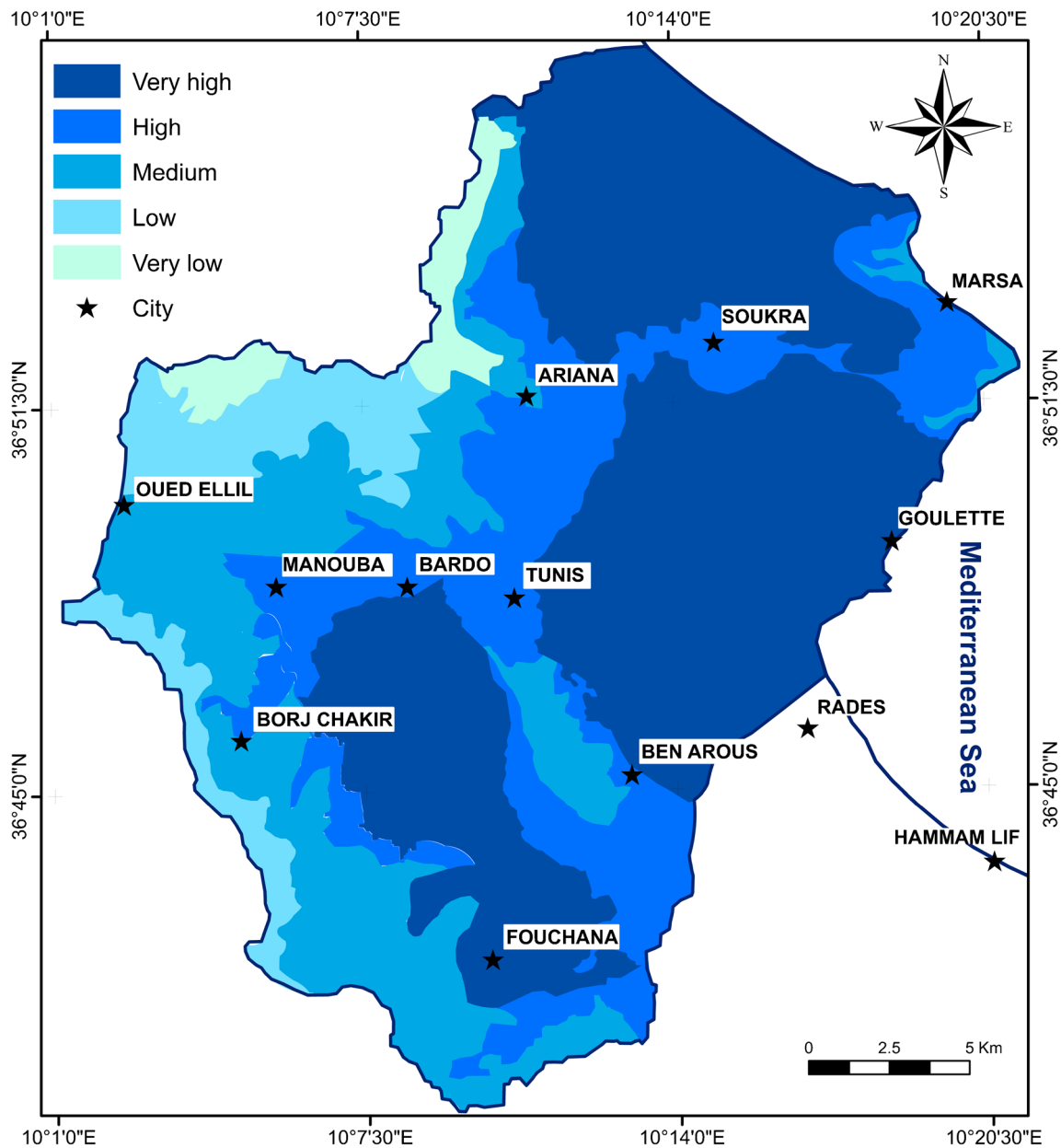
Fig. 8 Flood susceptibility map

Table 7 Statistics of the effective weights-sensitivity analysis

Factors	Theoretical weighting (°/°)	Effective weighting (°/°)		
		Mean	Min	Max
Land use/land cover (LULC)	23	30	4	38
Elevation (EL)	18	21	4	38
Lithology (LI)	18	18	4	38
Rainfall (RF)	15	14	8	38
Drainage density (DD)	10	7	8	38
Slope (SP)	8	4	4	38
Soil (SL)	5	5	8	38
Groundwater level (GL)	3	2	4	38

an efficient methodology to precise delineate the flood-susceptible areas. The spatial multicriteria decision analysis (MCDA) method was used in Tunisia to evaluate the effect of several factors, causing flood phenomenon generation, on the flood hazard occurences and the vulnerability of the flooding areas to each factor. This method analyzes spatially eight parameters such as land use/land cover, elevation, slope, lithology, drainage density, rainfall, soil, and groundwater level. The impact of each parameter on all other parameters was determined by applying the technique proposed by Shaban et al. (2001). Next, the MCDA approach is coupled with AHP techniques and GIS. GIS enhances here the visualization capability and increases the assessment efficiency, the acquisition, storage, retrieval, manipulation, and data analysis to develop information that can support decisions would be made in a shorter time. To estimate flood hazard, the influenced factors were fixed and their corresponding weights in accordance with flood formation were estimated, using analytic hierarchy process and pairwise comparison. This new approach does not require any training stage and it is easy to apply it. Moreover, it is applied to any regions. The main advantage of the method is the property given by the statement "depending on expert knowledge." However, this is also the main disadvantage. Expert subjectivity, particularly in pairwise comparisons, constitutes the main drawback of the AHP.

This study demonstrates that the land-use/land-cover factor is the main parameter of flooding. The highest weight was assigned to the land use-land cover parameter and the lowest weight to the groundwater level. This clarify that most floods occur due to human intervention to extensive urbanization and the natural torrential environment.

Flood susceptibility map in terms of natural and anthropogenic factors was constructed and classified into five major classes with flood potentiality from very low to very high. Respectively, we find 2.85% (very low), 7.5% (low), 17.95% (moderate), 20.63% (high), and 51.06% (very high). After that, FHI was coupled with a sensitivity analysis process to have a revised index FHIS. This index evaluates the impact of each criterion on the method, which leads to a better understanding of each parameter on the flood susceptibility map.

Finally, the produced maps from the current study can be used as a guide for flood management in the Tunis region. The knowledge about high-risk zones is important for local authorities to manage inundation properly in order to organize the implementation of the appropriate projects for flood protection.

References

Al-Adamat R, Foster I, Baban S (2003) Groundwater vulnerability and risk mapping for the basaltic aquifer of the Azraq basin of Jordan using GIS, remote sensing and DRASTIC. Appl Geogr 23:303–324

Althuwaynee OF, Pradhan B, Park HJ, Lee JH (2014) A novel ensemble bivariate statistical evidential belief function with knowledge-based analytical hierarchy process and multivariate statistical logistic regression for landslide susceptibility mapping. Catena 114:21–36

Akbari GH, Rahimi Shahrbabaki M (2011) Sensitivity analysis of water at higher risk subjected to soil contaminations. Comp Meth Civil Eng 2(1):73–90

Arrighi C, Brugioni M, Castelli F, Franceschini S, Mazzanti B (2018) Flood risk assessment in art cities: the exemplary case of Florence (Italy). J Flood Risk Manage 11:S616–S631

Ben ayed N, Bismuth H, Viguier N (1979) Présence de l'Oligocène dans les banlieues nord et sud-est de Tunis, Notes du Service Géologique de Tunis. Tunisie, n°45:55–70

Benson D, Lorenzoni I, Cook H (2016) Evaluating social learning in England flood risk management: an 'individual-community interaction'perspective. Environ Sci Pol 1(55):326–334

Boutib L (1998) Tectonique de la région du grand Tunis: Évolution géométrique et cinématique des blocs structuraux du Mésozoïque à l'actuel, Thèse de doctorat, Univ. Tunis, fac. Sci. Tunis, 151 p

Bujakka P, Rakus M, Vacek J (1971) Directorate of Mines and Energy. (Carte géologique de la Goulette à 1/50 000, feuille n° 21, Ministère de l'Economie Nationale. Direction des mines et de l'énergie)

Brivio PA, Colombo R, Maggi M, Tomasoni R (2010) Integration of remote sensing data and GIS for accurate mapping of flooded areas. Int J Remote Sens 23(3):429–441

Chabbi M, Abid H (2008) La mobilité urbaine dans le Grand Tunis, Évolutions et perspectives, rapport de projet, 94 p)

Chen Y, Liu R, Barrett D, Gao L, Zhou M, Renzullo L, Emlyanova I (2015) A spatial assessment framework for evaluating flood risk under extreme climates. Sci Total Environ 538:512–523

CRDA (2015) Commissariat Régionale au Développement Agricole du Gouvernorat de Tunis, Ariana, Ben arous et Manouba: Annuaires pluviométriques (1985–2015)

De Roo APJ (1999) LISFLOOD: a rainfall-runoff model for large river basins to assess the influence of land use changes on flood risk. In: Balabanis, P. et al. (Eds.), Ribamod: river basin modelling, management and flood mitigation. Concerted action, European Commission, EUR 18287 EN, pp. 349–357

DGRE (2015) Direction Générale des Ressources en Eau: Annuaires pluviométriques (1985–2015)

DHU (2015) Drection de l'Hydraulique Urbaine, 2015. Etude de protection contre les inondations du Grand Tunis. Tunisie, 463p

Drobne S, Lisec A (2009) Multi-attribute decision analysis in GIS: weighted linear combination and ordered weighted averaging. Informatica 33(4):459–474

Emberger L (1955) A biographical classification of climates. Rec Trav Lab Geol Bot Zool Fac Sci Montpellier 7:1–47

Elkhrachy I (2015) Flash flood hazard mapping using satellite images and GIS tools: a case study of Najran City, Kingdom of Saudi Arabia (KSA). National Authority for Remote Sensing and Space SciencesThe Egyptian Journal of Remote Sensing and Space Sciences 18(2):261–278

Farah EA, Abdulatif OM, Kheir OM, Baraz N (1997) Groundwater resources in a semi-arid area: a case study from central Sudan. J Afr Earth Sci 25(3):453–466

Forte F, Strobl R, Pennata L (2006) A methodology using GIS, aerial photos and remote sensing for loss estimation and flood vulnerability analysis in the Supersano-Ruffano-Nociglia Graben, southern Italy. Environ Geol 50(4):581–594

Fritch TG, McKnight CL, Yelderman JR, Arnold JG (2000) An aquifer vulnerability assessment of the Paluxy aquifer, central Texas, USA, using GIS and a modified DRASTIC approach. Environ Manag 25(3):337–345

Generino P, Sony E, Proceso LF (2014) Analytic hierarchy process (AHP) in spatial modeling for floodplain risk assessment. Int J Mach Learn Comput 4(5):450

Ghanbarpour MR, Salimi S, Hipel KW (2013) A comparative evaluation of flood mitigation alternatives using GIS-based river hydraulics modelling and multicriteria decision analysis. J Flood Risk Manag 6(4):319–331

Givisiez GHN, Oliveira EL (2009) Household size and demographic dividend in Brazilian housing market. IUSSP International Population Conference, p 2009

Gundogdu KS, Guney I (2007) Spatial analyses of groundwater levels using universal kriging. J Earth Syst Sci 116(1):49–55 http://www.ias.ac.in/article/fulltext/jess/116/01/0049-0055

Green CH, Parker DJ, Tunstall SM (2000) Assessment of flood control and management options. Thematic review IV.4 prepared as an input to the world commission on dams, Cape Town, http://www.dams.org

Hapuarachchi HAP, Wang QJ, Pagano TC (2011) A review ofadvances in flash flood forecasting. Hydrol Process 25:2771–2784. https://doi.org/10.1002/hyp.8040

Hanratty PJ, Joseph B (1992) Decision-making in chemical engineering and expert systems: application of the analytic hierarchy process to reactor selection. Comput Chem Eng 1 16(9):849–860

INS (2015) Recensement Général de la Population et de l'Habitat. Rebublique Tunisienne, 56p

INM (2015) Institut National de la Météorologie, Tableaux climatiques mensuels. Archive INM pour la période de 1985–2015.Tunis

Kaliraj S, Chandrasekar N, Magesh N (2014) Identification of potential groundwater recharge zones in Vaigai upper basin, Tamil Nadu, using GIS-based analytical hierarchical process (AHP) technique. Arab J Geosci 7(4):1385–1401

Kazakis N, Kougias I, Patsialis T (2015) Assessment of flood hazard areas at a regional scale using an index-based approach and analytical hierarchy process: application in Rhodope–Evros region, Greece. Sci Total Environ 538:555–563 http://www.sciencedirect.com/science/article/pii/S0048969715305581

Kourgialas NN, Karatzas G (2011) Flood management and a GIS modelling method to assess flood-hazard areas— a case study. Hydrological Sciences Journal–Journal des Sciences Hydrologiques 56(2):212–225

Lajmi T (1968) Contribution à l'étude géologique et hydrogéologique de la plaine du Mornag (Tunisie). Notes Serv Geol Tunisia, No. 27, 51 p., 13 Fig, 14 pl.

Liu YB, Gebremeskel S, De Smedt F, Hoffmann L, Pfister L (2003) A diffusive transport approach for flow routing in GIS-based flood modeling. J Hydrol 283(1–4):91–106

Matori AN, Lawal DU, Yusof KW, Hashim MA, Balogun A (2014) Spatial analytic hierarchy process model for flood forecasting: an integrated approach. Environ Earth Sci 20(1):012029

Maamri R, Ben Salem H (2000) Carte géologique de la Marsa 1/50 000, Edit. Serv Geol. From Tunisia

Meyer V, Becker N, Markantonis V, Schwarze R, Bergh J, Bouwer L, Bubeck P, Ciavola P, Genovese E, Green C, Hallegatte S, Kreibich H, Lequeux Q, Logar I, Papyrakis E, Pfurtscheller C, Poussin J, Przyluski V, Thieken A (2013) Assessing the costs of natural hazards—state of the art and knowledge gaps. Nat Hazards Earth Syst Sci 13(5):1351–1373

Magesh NS, Chandrasekar N, Soundranayagam JP (2012) Delineation of groundwater potential zones in Theni district, Tamil Nadu, using remote sensing, GIS and MIF techniques. Geosci Front 3(2):189–196

Murthy KSR (2000) Ground water potential in a semi-arid region of Andhra Pradesh-a geographical information system approach. Int J Remote Sens 21(9):1867–1884

Naik PK, Tamble JA, Dehury BN, Tiwari AN (2008) Impact of urbanization on the groundwater regime in a fast growing city in Central India. Environ Monit Assess 146(1–3):339–373

Nuissl H, Haase D, Lanzendorf M, Wittmer H (2009) Environmental impact assessment of urban land use transitions—a context-sensitive approach. Land Use Policy 26(2):414–424

Oikonomidis D, Dimogianni S, Kazakis N, Voudouris K (2015) A GIS/remote sensing based methodology for groundwater potentiality assessment in Tirnavos area, Greece. Journal of Hydrology 525: 197–208

Ortiz R, Ortiz P, Martín JM, Vázquez MA (2016) A new approach to the assessment of flooding and dampness hazards in cultural heritage, applied to the historic centre of Seville (Spain). Sci Total Environ 1(551):546–555

Oueslati A (1994) Les côtes de la Tunisie. Recherche sur leur évolution au Quaternaire. Imprimerie officielle de la République tunisienne, Tunis, 102p

Ogden FL, Raj Pradhan N, Downer CW, Zahner JA (2011) Relative importance of impervious area, drainage density, width function, and subsurface storm drainage on flood runoff from an urbanized catchment. Water Resour Res 47(12)

OTC (1980) Carte géologique de l'ariana à 1/50 000. Topography and Cartography Office

Pini S, Kchouk F (1971) Carte géologique de la Tunisie à 1/50 000, feuille d'Ariana, n°13)

Pini S (1971) Notice explicative de la carte géologique de Tunisie à 1/50 000, feuille d'Ariana, n°13, 62 p

Pourghasemi HR, Biswajeet P, Candan G (2012) Application of fuzzy logic and analytical hierarchy process (AHP) to landslide susceptibility mapping at Haraz watershed, Iran. Nat Hazards 63(2):965–996

Poussin JK, Botzen WW, Aerts JC (2014) Factors of influence on flood damage mitigation behavior by households. Environ Sci Pol 40:69–77

Pirdashti M, Ghadi A, Mohammadi M, Shojatalab G (2009) Multi-criteria decision-making selection model with application to chemical engineering management decisions. World Academy of Science. Eng Technol 49:54–59

Qiong L, Jianzhong Z, Donghan L, Xingwen J (2012) Research on flood risk analysis and evaluation method based on variable fuzzy sets and information diffusion. Saf Sci 50(5):1275–1283

Rahmati O, Haghizadeh A, Stefanidis S (2016a) Assessing the accuracy of GIS-based analytical hierarchy process for watershed prioritization; Gorganrood River Basin, Iran. Water resources management. Feb 1;30(3):1131–50

Rahmati O, Zeinivand H, Besharat M (2016b) Flood hazard zoning in yasooj region, Iran, using gis and multi-criteria decision analysis. Geomat Nat Haz Risk 73(3):1000_1017

Razandi Y, Pourghasemi HR, Neisani NS, Rahmati O (2015) Application of analytical hierarchy process, frequency ratio, and certainty factor models for groundwater potential mapping using GIS. Earth Sci Inf 8(4):867–883

Saaty TL (1980) The analytic hierarchy process: planning, priority setting, resource allocation. McGraw, New York, p 281

Senanayake D, Dissanayake B, Mayadunna W (2016) An approach to delineate groundwater recharge potential sites in Ambalantota, Sri Lanka using GIS techniques. Geosci J 7(1):115–124

Shaban A, Khawlie M, Kheir RB, Abdallah C (2001) Assessment of road instability along a typical mountainous road using GIS and aerial photos, Lebanon–eastern Mediterranean. Bull Eng Geol Environ. 1;60(2):93–101

Shaban A, Khawlie M, Abdallah C (2006) Use of remote sensing and GIS to determine recharge potential zones: the case of Occidental Lebanon. Hydrogeol J 14(4):433–443

Shankman D, Keim BD (2016) Flood risk forecast for China's Poyang Lake region. Phys Geogr. 2;37(1):88–91

Svoboda A (1991) Changes in flood regime by use of the modified curve number method. Hydrol Sci J 36(5):461–470

Stefanidis S, Stathis D (2012) Assessment of flood hazard based on natural and anthropogenic factors using analytic hierarchy process (AHP). Nat Hazards 68(2):569–585

Tehrany MS, Pradhan B, Jebur MN (2014) Flood susceptibility mapping using a novel ensemble weights-of-evidence and support vector machine models in GIS. J Hydrol 512:332–343

Thornthwaite CW, Mather JR (1957) Instructions and tables for computing potential evapotranspiration and the water balance (No. 551.57 T515i). Drexel Institute of Technology, Centerton, NJ (EUA). Laboratory of Climatology

Tucci CEM, Porto RLL, Barros MTD (1995) Inundações urbanas. Porto RL, Barros M.T (eds) Drenagem urbana. Universidade do Rio Grande do Sul. Porto Agere: ABRH/UFRGS. 429p

Troch PA, De Troch FP, Brutsaert W (1993) Effective water table depth to describe initial conditions prior to storm rainfall in humid regions. Water Resour Res 29(2):427–434

Upton KA, Jackson CR (2011) Simulation of the spatio-temporal extent of groundwater flooding using statistical methods of hydrograph classification and lumped parameter models. Hydrol Process 25(12):1949–1963

Ushiyama T, Kwak Y, Ledvinka O, Iwami Y, Danhelka J (2017) Interdisciplinary approach for assessment of continental river flood risk: a case study of the Czech Republic. In EGU General Assembly Conference Abstracts 19:5737

Van der Sande CJ, De Jong SM, De Roo AP (2003) A segmentation and classification approach of IKONOS-2 imagery for land cover mapping to assist flood risk and flood damage assessment. Int J Appl Earth Obs Geoinf. 1;4(3):217–229

Weng Q (2001) Modeling urban growth effects on surface runoff with the integration of remote sensing and GIS. Environ Manag 28(6):737–748

Wang Y, Li Z, Tang Z, Zeng G (2011) A GIS-based spatial multi-criteria approach for flood risk assessment in the Dongting Lake Region, Hunan, Central China. Water Resour Manag 25(13):3465–3484

Yang M, Qian X, Zhang Y, Sheng J, Shen D, Ge Y (2011) Spatial multicriteria decision analysis of flood risks in Aging-Dam Management in China: a framework and case study. Int J Environ Res Publ 8(5):1368–1387

Yaralıoğlu K (2004) Analitik Hiyerarşi Proses. Uygulamada Karar Destek Yöntemleri. İlkem Ofset, İzmir

Youssef A, Pradhan B, Hassan A (2011) Flash flood risk estimation along the St. Katherine road, southern Sinai, Egypt using GIS based morphometry and satellite imagery. Environ Earth Sci 62(3):611–623

Yahaya S (2008) Multi criteria analysis for flood vulnerable areas in Hadejia-Jama'Area river basin, Nigeria ASPRS Annual conference Portland

Zghibi A, Merzougui A, Chenini I, Ergaieg K, Zouhri L, Tarhouni J (2016) Groundwater vulnerability analysis of Tunisian coastal aquifer: an application of DRASTIC Index Method in GIS environment. Groundw Sustain Dev 2:169–181